Thermodynamic properties near the onset of loop-current order in high-T_c superconducting cuprates

M. S. Grønsleth,[1] T. B. Nilssen,[1] E. K. Dahl,[1] E. B. Stiansen,[1] C. M. Varma,[2] and A. Sudbø[1]
[1]*Department of Physics, Norwegian University of Science and Technology, N-7491 Trondheim, Norway*
[2]*Department of Physics and Astronomy, University of California, Riverside, California 92521, USA*
(Received 10 July 2008; published 4 March 2009)

We have performed large-scale Monte Carlo simulations on a two-dimensional generalized Ashkin-Teller model to calculate the thermodynamic properties in the critical region near its transitions. The Ashkin-Teller model has a pair of Ising spins at each site which interact with neighboring spins through pair-wise and four-spin interactions. The model represents the interactions between orbital current loops in CuO_2 plaquettes of high-T_c cuprates, which order with a staggered magnetization M_s inside each unit cell in the underdoped region of the phase diagram below a temperature $T^*(x)$ which depends on doping. The pair of Ising spins per unit cell represents the directions of the currents in the links of the current loops. The generalizations are the inclusion of anisotropy in the pair-wise nearest-neighbor current-current couplings consistent with the symmetries of a square lattice and the next-nearest-neighbor pair-wise couplings. We use the Binder cumulant to estimate the correlation length exponent ν and the order-parameter exponent β. Our principal results are that in a range of parameters; the Ashkin-Teller model as well as its generalization has an order-parameter susceptibility which diverges as $T \to T^*$ and an order parameter below T^*. Importantly, however, there is no divergence in the specific heat. This puts the properties of the model in accord with the experimental results in the underdoped cuprates. We also calculate the magnitude of the "bump" in the specific heat in the critical region to put limits on its observability. Finally, we show that the staggered magnetization couples to the uniform magnetization M_0 such that the latter has a weak singularity at T^* and also displays a wide critical region, also in accord with recent experiments.

DOI: 10.1103/PhysRevB.79.094506 PACS number(s): 74.20.Rp, 74.50.+r

I. INTRODUCTION

It has been proposed[1,2] that the properties of the cuprate compounds are controlled by the onset of a time-reversal and inversion violating order parameter below a temperature $T = T^*(x)$, which depends on the doping x. $T^*(x) \to 0$ for $x \to x_c$ in the superconducting range of compositions, thus defining a quantum critical point. The quantum critical fluctuations associated with the breakup of the specific order proposed was shown[3] to be of the scale-invariant form hypothesized to lead to a marginal Fermi liquid,[4] which explains the anomalous transport properties of these compounds. $T^*(x)$ is identified with the observed onset of the pseudogap properties in the cuprates.

A major difficulty in accepting these ideas is that there is no observed specific-heat divergence near $T^*(x)$ in any cuprate. On the other hand, there now exists significant evidence for long-range order with a spatial symmetry consistent with orbital currents of the form shown in Fig. 1 in three different families of cuprates[5–8] which have been investigated so far. There is also evidence of a weak singularity at $T^*(x)$ in the uniform magnetic susceptibility.[9]

In view of this situation, it is important to investigate whether or not the proposed models for these broken symmetries are consistent simultaneously with long-range order without an observable signal in the specific heat in the measurements made hitherto, and also whether it does give rise to observable features in the uniform magnetization induced by an external magnetic field.[9]

The particular form of proposed hidden order is one of spontaneously generated fluxes in the O-Cu-O plaquettes of the CuO_2 unit cell such that currents flow in two oppositely directed loops in each unit cell, as depicted for one of the four possible domains in Fig. 1. (See also Fig. 1 of Refs. 2 and 10.) The *staggered* orbital magnetic moments within

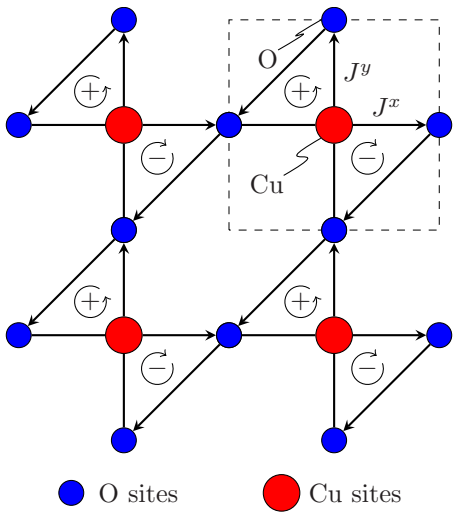

FIG. 1. (Color online) The circulating current phase Θ_{II} (Ref. 2). The Cu sites are red (large) circles while O sites are blue (small) circles. The unit cell is shown by the dashed square. A staggered magnetic-moment pattern within each unit cell that repeats from unit cell to unit cell (the curl of the directed circles) is indicated. The currents J^x and J^y represent the horizontal and vertical currents, respectively, to be used in the derived effective model [Eq. (1)]. Physically, they represent the *coherent parts* of the orbital fermionic currents in the problem.

each CuO_2 unit cell repeats from unit cell to unit cell so that the translational symmetry of the lattice remains unaltered. These circulating current patterns are generated by a nearest-neighbor repulsion V between Cu and O atoms in the CuO_2 sheets. The effect of such a repulsive V term has been extensively investigated in one-dimensional (1D) CuO chains, where it has been shown to drive charge-transfer instabilities and superconductivity.[11–13] In Ref. 14, the existence of current-loop ordering was not confirmed but the work was carried out on a truncated effective $t-J$ model of eight Cu sites. Moreover, the ground state was spin polarized with finite momentum, which would not be representative of the large-scale physics of interest in the system. The truncation of the Hilbert space used in Ref. 14 furthermore requires much large values of onsite Coulomb repulsion on oxygen sites that it is probably outside the parameter regime of the high-T_c cuprates.[15] This motivated the authors of Ref. 16 to undertake a large-scale study of the issue of current-loop ordering on much larger systems using the full three-band model of the CuO_2 planes via variational Monte Carlo simulations. These authors found clear evidence for current-loop ordering. Other types of current patterns and charge fluctuations are also possible.[1,17,18]

II. FUNDAMENTALS

In this section, we present the effective model of fluctuating orbital currents that we studied in this paper, along with the definitions of the thermodynamic quantities we computed, as well as some remarks on the critical exponents of the problem with emphasis on the particular status of the specific-heat exponent of the problem at hand.

A. Model

The effective model we performed Monte Carlo simulations on has been derived from a microscopic description of the CuO_2 planes of high-T_c cuprates elsewhere.[10,19] It turned out to be a generalization of the model initially proposed to describe the statistical mechanics of loop-current order[2,3] in which some terms allowed by symmetry were omitted. The action S is written in the form $S=S_C+S_Q$, where S_C is the classical piece of the action, and S_Q is part of the action that is needed in the quantum domain of the theory. In this paper, we will focus on discussing the effects of thermal fluctuations, and we will therefore not need S_Q. The classical part of the action, S_C, is given by[10,19]

$$S_C = -\beta \sum_{\langle \mathbf{r},\mathbf{r}' \rangle} (K_x J^x_{\mathbf{r}} J^x_{\mathbf{r}'} + K_y J^y_{\mathbf{r}} J^y_{\mathbf{r}'}) - \beta \sum_{\langle\langle \mathbf{r},\mathbf{r}' \rangle\rangle} K^{xy}_{\mathbf{r}\mathbf{r}'} (J^x_{\mathbf{r}} J^y_{\mathbf{r}'} + J^y_{\mathbf{r}} J^x_{\mathbf{r}'}) - \beta K_4 \sum_{\langle \mathbf{r},\mathbf{r}' \rangle} J^x_{\mathbf{r}} J^x_{\mathbf{r}'} J^y_{\mathbf{r}} J^y_{\mathbf{r}'}. \quad (1)$$

Here, $\langle \mathbf{r},\mathbf{r}' \rangle$ and $\langle\langle \mathbf{r},\mathbf{r}' \rangle\rangle$ denote nearest-neighbor and next-nearest-neighbor summations, respectively. $\beta=1/T$, where T is temperature, and we work in units where Boltzmann constant $k_B=1$. We will only consider the directions $\pm$ of the current variables $J^{x,y}$, assuming as in other similar two-dimensional (2D) models that their amplitudes are smoothly varying with temperature and do not determine the critical properties. Note that there is always also a current in the O-O links whose magnitude is equal to that of J^x which has the same magnitude as J_y. Therefore, no current flows out of any O-Cu-O triangular plaquette. Due to the restriction that no current flows out of any O-Cu-O plaquette, there is no need to specify the O-O currents. The variables J^x and J^y are then the same as the $\sigma=\pm 1$ and $\tau=\pm 1$ Ising variables introduced earlier.[3] Fluctuations $(J^x_{\mathbf{r}} \to -J^x_{\mathbf{r}}, J^y_{\mathbf{r}} \to J^y_{\mathbf{r}})$ corresponds to going from the depicted current pattern (Fig. 1) to a new one which is obtained by a counterclockwise rotation by $\pi/2$, $(J^x_{\mathbf{r}} \to J^x_{\mathbf{r}}, J^y_{\mathbf{r}} \to -J^y_{\mathbf{r}})$ corresponds to clockwise rotation of $\pi/2$, and $(J^x_{\mathbf{r}} \to -J^x_{\mathbf{r}}, J^y_{\mathbf{r}} \to -J^y_{\mathbf{r}})$ to a rotation of π.

If one ignores the next-nearest-neighbor terms and takes $K_x=K_y$, one gets the Ashkin-Teller (AT) model,[20] for which several exact results are known[21] asymptotically close to the phase-transition lines. However, since the currents are bond variables, one necessarily has an anisotropy in the nearest-neighbor interactions,[10,19] such that for $\mathbf{r}-\mathbf{r}'=\pm\hat{\mathbf{x}}$, $K_x=K_l$ and $K_y=K_t$, whereas when $\mathbf{r}-\mathbf{r}'=\pm\hat{\mathbf{y}}$, $K_x=K_t$ and $K_y=K_l$. It is important to investigate whether this anisotropy is an *irrelevant* perturbation. We will in the following denote the anisotropy by the parameter $A \equiv K_t/K_l$. Similarly, it is interesting to investigate the effect of the next-nearest-neighbor interaction given by the parameter $K^{xy}_{\mathbf{r}\mathbf{r}'}=K^{xy}$, when $\mathbf{r}-\mathbf{r}' = \pm(\hat{\mathbf{x}}+\hat{\mathbf{y}})$ and $K^{xy}_{\mathbf{r}\mathbf{r}'}=-K^{xy}$ when $\mathbf{r}-\mathbf{r}'=\pm(\hat{\mathbf{x}}-\hat{\mathbf{y}})$.

Let us comment briefly on the terms appearing to quartic order, most of which either are constants or renormalize the quadratic piece of the action. Note that four Ising variables of two distinct species all located on one single lattice site simply contribute a constant to the action. If we now limit ourselves to terms that have four J fields distributed on two nearest-neighbor lattice sites, only two distinct possibilities exist. First, we may have a term with three J's on one lattice site and one J on a nearest-neighbor site. This merely represents a renormalization of the quadratic couplings. Second, we may have two J's on one lattice site and another two on a nearest-neighbor lattice site. Unless there are two distinct species of J's on each of the lattice sites, such a term will represent a constant contribution to the action. If the J's on each lattice site are of distinct species, the term will be of the AT form, as written above. We will ignore terms that have J fields distributed on three or four distinct lattice sites, such as for instance plaquette terms, as these are generated by much higher order terms.[10,19]

B. Thermodynamic quantities

In this paper, we calculate the evolution of the specific heat, the staggered orbital magnetic moment, as well as the susceptibility of the staggered orbital magnetic moment as we vary K_4 in Eq. (1). We also perform finite-size scaling on the magnetization and the Binder cumulant (see below). The specific heat C_v is given by

$$C_v = \frac{1}{L^2} \langle (\mathcal{S}_C - \langle \mathcal{S}_C \rangle)^2 \rangle. \quad (2)$$

Considering Fig. 2, we see that we may define a "pseudospin" $\mathbf{S}$ on each lattice given by $\mathbf{S}_{\mathbf{r}} \equiv (J^x_{\mathbf{r}}, J^y_{\mathbf{r}})$. The various

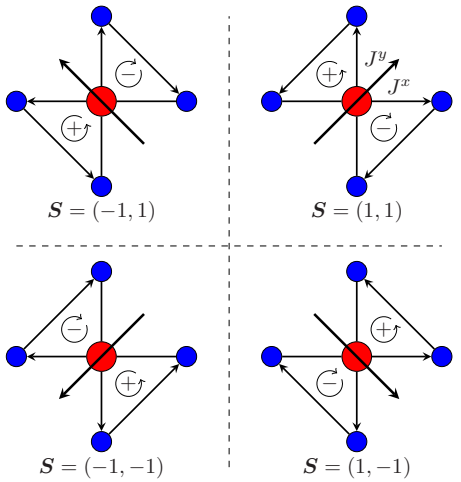

FIG. 2. (Color online) An illustration of the pseudospin $\mathbf{S}=(J^x_{\mathbf{r}},J^y_{\mathbf{r}})$ we used to compute the staggered order parameter and its susceptibility [Eqs. (3) and (4)].

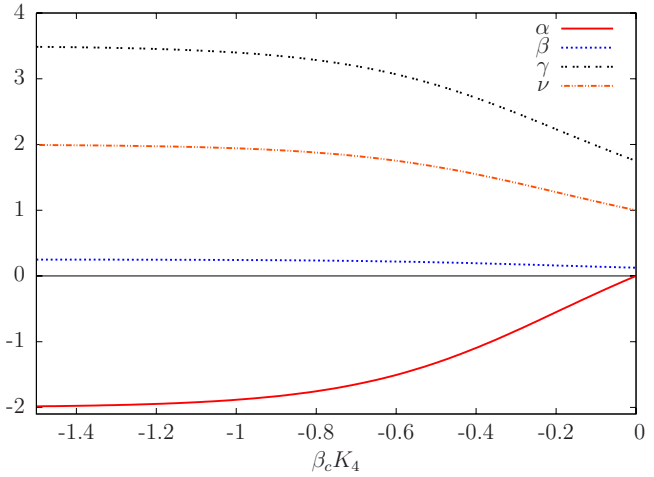

FIG. 3. (Color online) Critical exponents α, β, and γ from the Ashkin-Teller model, as a function of the four-spin coupling $\beta_c K_4 \leq 0$ (Ref. 21). In this parameter range, we have $-2<\alpha\leq 0$, $1/8 \leq \beta < 1/4$, $7/4 \leq \gamma < 7/2$, and $1 \leq \nu < 2$.

states of the system are then described by a four-state clock pseudospin $\mathbf{S}_{\mathbf{r}}=(\pm 1,\pm 1)$ on a two-dimensional square lattice. We define the staggered order parameter in the standard way it would be defined for a clock model, namely,

$$\langle M_s\rangle \equiv \frac{1}{L^2}\left\langle \sqrt{\frac{(m^x)^2+(m^y)^2}{2}}\right\rangle, \tag{3}$$

where $m^\alpha \equiv \Sigma_{\mathbf{r}} J^\alpha_{\mathbf{r}}$, $\alpha \in (x,y)$. The susceptibility of this staggered order parameter is given by

$$\chi_s = \frac{1}{2L^2T}[\langle (m^x)^2+(m^y)^2\rangle - \langle\sqrt{(m^x)^2+(m^y)^2}\rangle^2]. \tag{4}$$

We will contrast the singularities in these quantities with the evolution of the anomaly in the specific heat as the parameter K_4 is varied. While the above staggered moment does not couple linearly to an external uniform magnetic field, it couples to a field-induced uniform magnetic moment via a quartic term in the free energy. The field-induced uniform magnetization must therefore have a nonanalytic behavior across the phase transition where the staggered magnetization associated with the ordering of the orbital currents sets in. We will return to this point in Sec. IV.

For the purposes of extracting the critical exponent ν, we consider the Binder cumulant, defined by

$$G \equiv \frac{\langle m^4\rangle}{\langle m^2\rangle^2}, \tag{5}$$

where $m^2=(m^x)^2+(m^y)^2$, corresponding to the magnetization order parameter $\langle|\mathbf{m}|\rangle$, whose critical exponent β is given in Eq. (6) for the AT model.[21] In the ordered phase, $G=1$. For an N-component order parameter, $G=(N+2)/N$ in the disordered phase. In our case, therefore, G will exhibit a rise from one to two as the systems disorder. When computing this quantity for different L and plotting it as a function of T, the curves should in principle cross at the same point, thus defining T_c. On the other hand, plotting it as a function of $L^{1/\nu}|(T-T_c)/T_c)|$, all the curves will collapse on top of each other. By adjusting ν to get data collapse, one obtains the correlation length exponent. Furthermore, the order-parameter exponent β is obtained from the magnetization M_s for various system sizes by considering the quantity $L^{\beta/\nu}M_s$, and adjusting β and ν so as to obtain data collapse when plotting this quantity as a function of $L^{1/\nu}|(T-T_c)/T_c)|$.

C. Critical exponents

Note that, although the K_x and K_y couplings between the two different types of Ising fields in this model are anisotropic,[10,19,22] there is only one (doubly degenerate Ising) phase transition in the system for $K^{xy}=0$; $K_4=0$. Hence, as the four-spin coupling K_4 is changed from zero, the Ising critical point evolves into a single phase-transition line with nonuniversal critical exponents.[21] In particular, the specific-heat exponent α becomes negative, with the transition line itself being a self-dual critical line.[21] In this sense, the model is similar to an *isotropic* AT model, where the exact result for the critical exponents are known, and given by[21]

$$\alpha = \frac{2-2y}{3-2y}; \quad \beta = \frac{1}{8}\left(\frac{2-y}{3-2y}\right). \tag{6}$$

From this, we deduce the susceptibility exponent $\gamma=14\beta$ and the correlation length exponent $\nu=8\beta$ from standard scaling relations. Note that the ratios $\gamma/\nu=7/4$ and $\beta/\nu=1/8$ are universal and independent of y. (It is also interesting to note that the anomalous scaling dimension $\eta=1/4$ and the magnetic field exponent $\delta=15$, precisely as in the 2D Ising model). Here $y=2\mu/\pi$ and $\cos(\mu)=[e^{4K_4/T_c}-1]/2$.[21] Hence, for $K_4\leq 0$, we have $\pi/2\leq\mu<2\pi/3$, such that $1\leq y<4/3$.

These exponents are plotted in Fig. 3. The most extreme deviation from the 2D Ising values $\alpha=0$, $\beta=1/8$, $\gamma=7/4$, and $\nu=1$ is given by the case $K_4\to-\infty$ and $y=4/3$, where $\alpha=-2$, $\beta=1/4$, $\gamma=7/2$, and $\nu=2$. Note the *increase* in γ and ν, (which implies a weak increase in β for increasing $-K_4$ due to the proportionality factors 14 and 8 given below Eq.

(6)) while we have a *substantial reduction* in α to *negative* values as $-K_4$ increases. This is traceable to the numerator $2-2y$ in α compared to the numerator $2-y$ in β, γ, and ν (while η and δ are independent of y). Hence, the specific-heat exponent stands out as very special in model Eq. (1). This fact is by far the single most dramatic difference between the critical behavior of Eq. (1) and the 2D Ising model. The K_4 term with $K_4<0$ simultaneously *suppresses* singularities in the specific heat, and *enhances* singularities both in the susceptibility corresponding to the staggered orbital magnetization of Fig. 1 and in the one associated with a field-induced uniform magnetization (see Sec. IV).

III. MONTE CARLO RESULTS

The Monte Carlo computations were performed using the standard single-spin update Metropolis-Hastings algorithm,[23,24] making local updates of the Ising fields $J^x_{\mathbf{r}}$ and $J^y_{\mathbf{r}}$, as well as local updates of the composite Ising field $J^x_{\mathbf{r}}J^y_{\mathbf{r}}$ at each lattice site. The system grid is defined by two two-dimensional subgrids, one for each Ising field, and the local updates were performed for all points on the grid. All the Ising fields on both subgrids were initially set to one. We started all simulations at the high-temperature end, and discarded the first 100 000 sweeps for the purpose of initially thermalizing the system. After that, measurements were made for every 100 sweeps. The system sizes that were considered were $L\times L$ with $L=64,128,256,512$. For each value of T, we ran up to 3×10^6 MC sweeps for $L=64,128,256$, and sampled the system for every 100 MC sweeps over the lattice, while we used 5×10^6 MC sweeps for $L=512$ and sampled the system for every 150 MC sweeps over the lattice. We have checked that satisfactory convergence is well established by the time we get to system sizes of $L=512$, and we therefore largely present results for these largest systems only, apart from Fig. 6 and the finite-size scaling results that will be presented for the Binder cumulant (see below). In all simulations, we have set $K_l=1.0$, such that all other couplings are measured relative to this parameter. In these units, the critical temperature T_c of the system for $A=1.0$, $K^{xy}=0$, and $K_4=0$ is given by $T_c=2/\ln(1+\sqrt{2})\approx2.27$. This sets the scale of the critical temperatures in the plots we will show below.

A. Specific heat

Let us first investigate what effect K^{xy} has on the logarithmic singularity of the 2D Ising model. In Fig. 4, we show the specific heat for $A=1.0$ and $K_4=0$, upon varying $K^{xy}=0.0,0.1,0.2,0.3$. We have limited the variations in K^{xy} because it can be shown in mean-field calculations that the order parameter changes the translational symmetry for large enough K^{xy} and a diagonal "striped" order is favored. It is seen that the K^{xy} term in this parameter range leaves the logarithmic singularity of the anisotropic double-Ising model [Eq. (1) with $K^{xy}=0$ and $K_4=0$] unaltered, only the amplitude of the singularity is changed.

We now investigate the effect of four-spin interactions $\propto K_4$. We will only consider negative values of K_4 in this

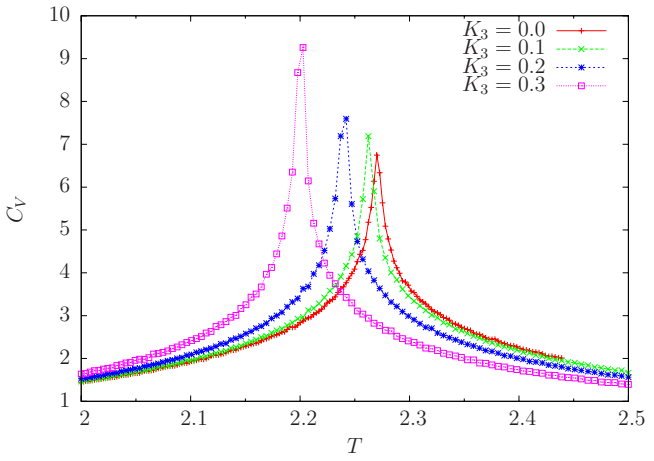

FIG. 4. (Color online) Specific heat as a function of temperature T for the classical part of the model in Eq. (1), with $A=1.0$ and $K_4=0.0$, for various values of $K^{xy}=0.0,0.1,0.2,0.3$, and system size $L=512$. The amplitude of the logarithmic specific heat of the Ising model ($K^{xy}=0$) is enhanced as K^{xy} increases but the anomaly remains logarithmic. The critical temperature of the 2D pure Ising model is given by $T_c=2/\ln(1+\sqrt{2})\approx2.27$ in units where Boltzmann constant $k_B=1$. Note also that for this set of parameters, K^{xy} hardly alters T_c of the model with $K^{xy}=0$.

paper. Then the four-spin term tends to promote a nonuniform ground state with antiferromagnetic ordering in the composite variable $J^x_{\mathbf{r}}J^y_{\mathbf{r}}$, thus frustrating the Ising terms in Eq. (1). It is known from the phase diagram of the AT model[20] that the ordered phase has a different symmetry in the regions $-1<K_4/K_l<1$, $K_4/K_l<-1$, and $K_4/K_l>1$. The region of special interest is $-1<K_4/K_l<0$ in which the AT model has a self-dual line of critical points.[25,26] This is consistent with the microscopic model, which may exhibit a negative sign of the four-spin interaction term.

We first consider the case of isotropic Ising coupling $K_l=K_t$, i.e., $A=1.0$, next-nearest-neighbor coupling $K^{xy}=0.0$, and increasing $|K_4|$. We use this case for reference, as this parameter set represents the standard isotropic AT model.[3,20] The results for the specific heat are shown in Fig. 5. The logarithmic specific heat of the Ising model disappears to be replaced by a bump whose extent in T increases as $|K_4|$ increases. This is consistent with the asymptotic critical exponents.[20]

In Fig. 6, we investigate how well these results are converged when increasing the system size through the values $L=64,128,256,512$. It is seen that the results appear well converged when L has reached 256, in particular the double-peak structure in C_V that is present for small system sizes disappears upon increasing L. In contrast to the Binder cumulant (see below), we have not attempted a data collapse of the specific heat by trying a scaling form $C_V(T,L)=L^{\alpha/\nu}\mathcal{C}_{\pm}[L^{1/\nu}(T-T_c)/T_c]$ and adjusting α to obtain data collapse. The reason is that we anticipate a negative specific-heat exponent, such that corrections to the above scaling form will be large, thus preventing data collapse. Even for positive α, it is well known that corrections to scaling are substantial for the specific heat. This simply means that the specific heat by itself oddly enough is not a very useful quan-

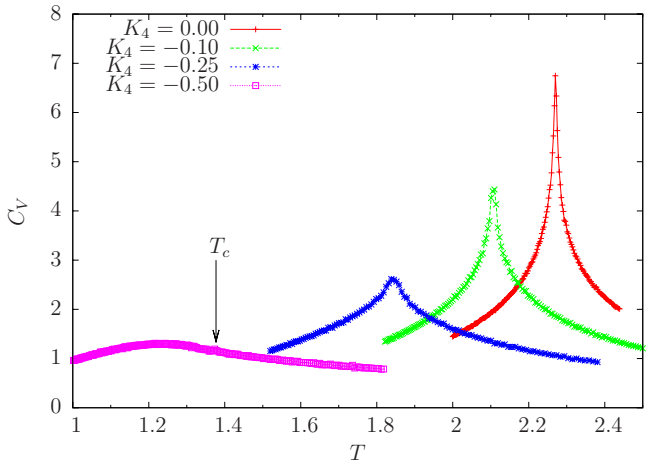

FIG. 5. (Color online) Specific heat as a function of temperature T for the classical part of generalized AT model Eq. (1), with $A=1.0$ and $K^{xy}=0.0$, for various values of $K_4=0.0,-0.1,-0.25,-0.5$, and system size $L=512$. The vertical scale is in units of k_B/unit cell. The logarithmic specific-heat singularity of the Ising model ($K_4=0$) is eliminated and replaced by a bump whose width increases as $|K_4|$ increases. The arrow in the lower right panel indicates T_c as obtained from the peak in the susceptibility χ_s.

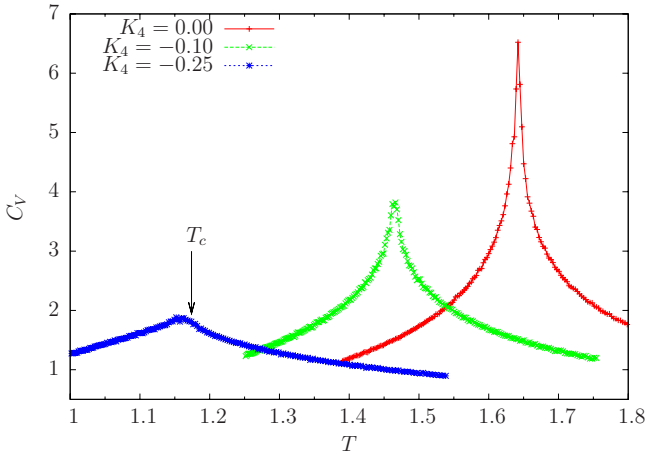

FIG. 7. (Color online) Specific heat as a function of temperature T for the classical part of generalized AT model Eq. (1), with $A=0.5$ and $K^{xy}=0.0$, for various values of $K_4=0.0,-0.1,-0.25$, and system size $L=512$. The vertical scale is in units of k_B/unit cell. Compared to the case shown in Fig. 5, with $A=1.0$, precisely the same trends are seen in the evolution of the anomaly as the AT coupling $|K_4|$ is increased, only slightly more pronounced. The arrow indicates T_c as obtained from the peak in the susceptibility χ_s.

tity from which to extract precise values of α in Monte Carlo computations on practical system sizes. Other techniques are required for this, see, e.g., Ref. 27. However, the main point of the present paper is not to determine a precise value of α numerically but rather to demonstrate (including all corrections to scaling) that a striking suppression of the prominent logarithmic singularity of the 2D Ising model takes place as $|K_4|$ is increased. Figure 6 clearly shows that the suppression is not a finite-size artifact. Note in particular that the relative height of the bump in C_V for nonzero $|K_4|$ is suppressed

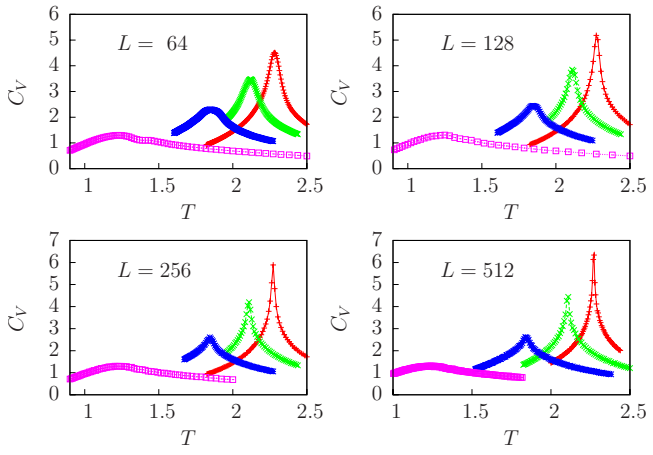

FIG. 6. (Color online) Specific heat as a function of temperature T for the classical part of generalized AT model Eq. (1), with $A=1.0$ and $K^{xy}=0.0$, for various values of $K_4=0.0,-0.1,-0.25,-0.5$, and system size $L=64,128,256,512$. The vertical scale is in units of k_B/unit cell. The logarithmic specific-heat singularity of the Ising model ($K_4=0$), is eliminated and replaced by a bump whose width increases as $|K_4|$ increases. Note how the double bump in C_V, which is present at smaller system sizes, disappears when L is increased. When $L=512$, the results appear to be well converged.

compared to the Ising singularity as L increases.

We next consider the effect of increasing the anisotropy ($A<1$), such as to weaken the ordering in each of the $J_y(\mathbf{r})$ and $J_x(\mathbf{r})$ Ising fields. Note that, however, because the anisotropy introduced is equal for both of the Ising fields (only the direction of the anisotropy is changed), the model only has one single critical point even in the absence of a K_4 coupling. The model is then merely two copies of one and the same anisotropic 2D Ising model. However, an increase in $|K_4|$ is expected to have a stronger effect for $A<1.0$ than when $A=1.0$ due to the weaker ordering and reduced critical temperature. The bump in the specific heat is then accordingly smoother as seen in Fig. 7 compared to Fig. 5.

We now repeat the above computations for $A=1.0$ with $K^{xy}=0.1$, 0.2, and 0.3. This coupling tends to frustrate the Ising ordering since a large K^{xy} tends to promote striped order due to the diagonal anisotropy (represented by a change in sign in K^{xy} upon $\pi/2$ rotations of next-nearest-neighbor vectors). It is of interest to see how the presence of K^{xy} affects the introduction of the AT coupling K_4. Naively, since the coupling K^{xy} promotes striped order and frustrates the uniform order promoted by K_x and K_y, we would expect that the suppressed anomalies are pushed to lower temperatures as K^{xy} is increased. In Figs. 8–10, we show the specific heat for the same sets of parameters as in Fig. 5 except that now $K^{xy}=0.1,0.2,0.3$, respectively.

We see that the effect of K^{xy} is to increase the sharpness of the bump in the specific heat while the effect of K_4 again is to widen the bump (in the presence of K^{xy}). We also see that the anomalies that remain are pushed slightly downwards in temperature compared to the case $K^{xy}=0$ (cf. the results of Fig. 5). The change is however only minor for the cases $K^{xy}=0.1$ and $K^{xy}=0.2$, consistent with the weak suppression of the critical temperature we found upon increasing K^{xy} at $K_4=0$ in Fig. 4. The conclusion we draw from these

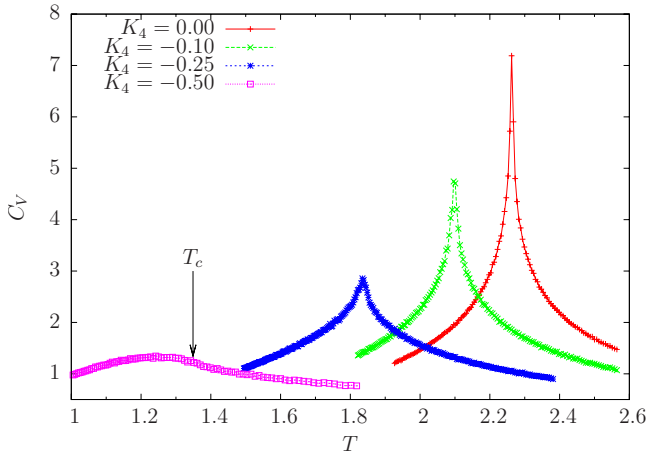

FIG. 8. (Color online) Specific heat as a function of temperature T for the classical part of generalized AT model Eq. (1), with $A=1.0$ and $K^{xy}=0.1$, for various values of $K_4=0.0,-0.1,-0.25,-0.5$, and system size $L=512$. The arrow indicates T_c as obtained from the peak in the susceptibility χ_s. The vertical scale is in units of k_B/unit cell.

computations is that the singularity of the specific heat of the Ising case is removed by the coupling K_4 is included. The resulting bump in the specific heat becomes sharper for increasing K^{xy} at finite K_4.

Finally, we consider the most general case of anisotropic Ising coupling $A=0.5$ and finite $K^{xy}=0.3$, as $|K_4|$ is increased, shown in Fig. 11.

It is clear from Fig. 11 that the introduction of anisotropy $A=K_t/K_l=0.5$ widens the width of the bump in the specific heat. This is easily understood since increasing anisotropy implies that the magnitude of K_4 relative to the Ising couplings in the problem will increase. The effect of a given increase in K_4 is therefore more strongly felt. Moreover, as in the isotropic case, the anomalies are pushed down in temperature compared to the case $K^{xy}=0$ (cf. the results of Fig. 7).

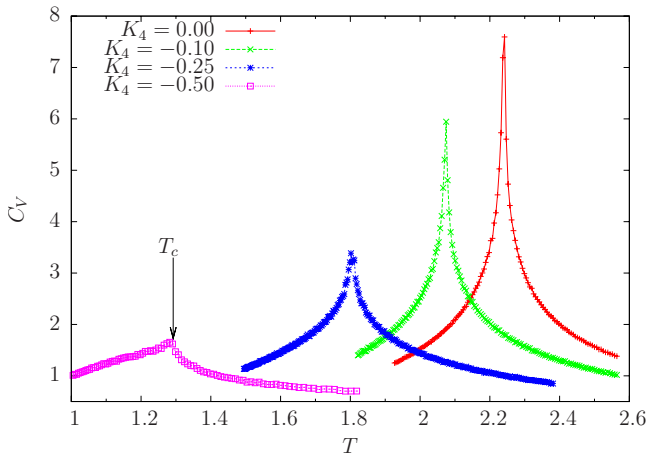

FIG. 9. (Color online) Specific heat as a function of temperature T for the classical part of generalized AT model Eq. (1), with $A=1.0$ and $K^{xy}=0.2$, for various values of $K_4=0.0,-0.1,-0.25,-0.5$, and system size $L=512$. The arrow indicates T_c as obtained from the peak in the susceptibility χ_s. The vertical scale is in units of k_B/unit cell.

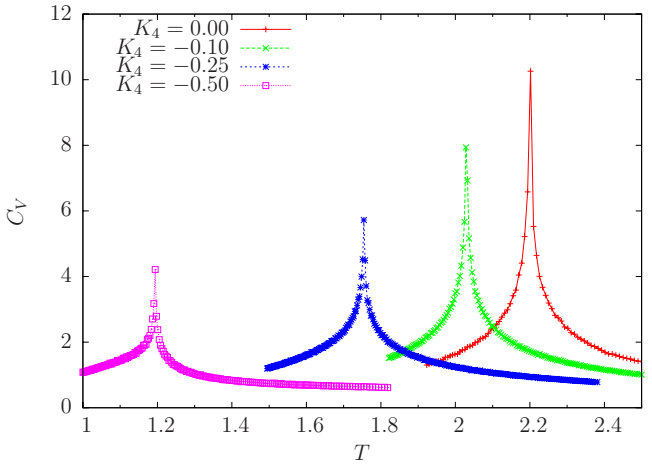

FIG. 10. (Color online) Specific-heat anomaly as a function of temperature T for the classical part of generalized AT model Eq. (1), with $A=1.0$ and $K^{xy}=0.3$, for various values of $K_4=0.0,-0.1,-0.25,-0.5$, and system size $L=512$. The vertical scale is in units of k_B/unit cell.

Concluding this section on the results for the specific heat, we mention that we have also, at the early stages of this work, performed a rather rudimentary comparative study of the specific-heat anomaly in the 2D Ashkin-Teller model and the 2D *XY* continuous rotor model with a four-fold symmetry-breaking term, on lattice sites up to $L=32$. This numerics is insufficient to draw any conclusions about the fluctuation spectrum on the disordered side of the transition, close to the transition, as the symmetry-breaking field becomes small. That is, the simulations per se do not allow us to conclude anything about the perturbative relevance or irrelevance of the symmetry-breaking term. What we have been able to confirm is that the specific-heat anomaly of the 2D Ashkin-Teller model is indistinguishable from the 2D *XY*

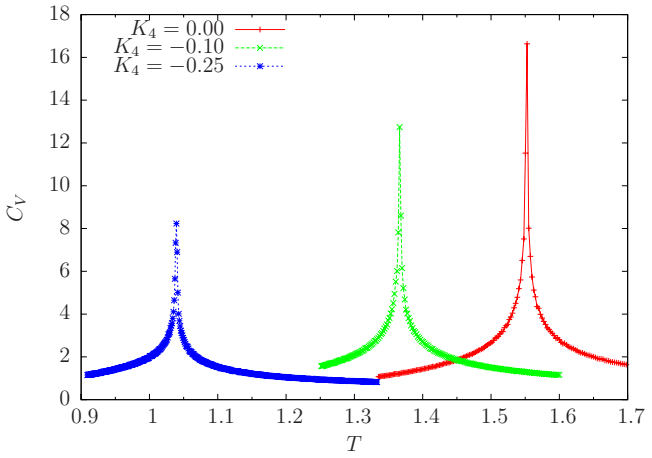

FIG. 11. (Color online) Specific-heat anomaly as a function of temperature T for the classical part of generalized AT model Eq. (1), with $A=0.5$ and $K^{xy}=0.3$, for various values of $K_4=0.0,-0.1,-0.25$, and system size $L=512$. The vertical scale is in units of k_B/unit cell.

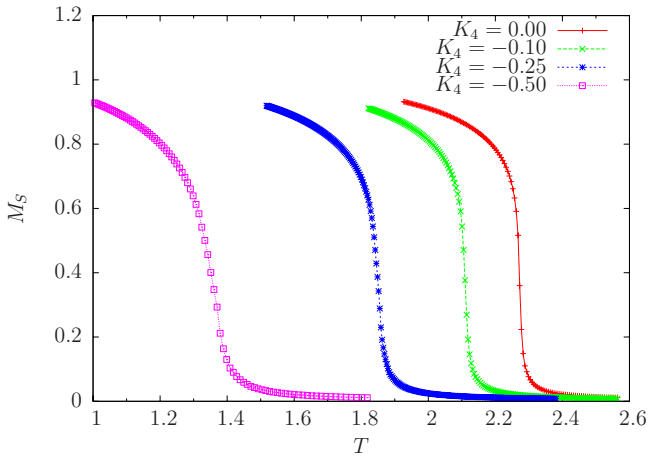

FIG. 12. (Color online) The staggered order parameter, Eq. (3), as a function of temperature T for the classical part of generalized AT model Eq. (1), with $A=1.0$ and $K^{xy}=0.0$, for various values of $K_4=0.0,-0.1,-0.25,-0.5$, and system size $L=512$.

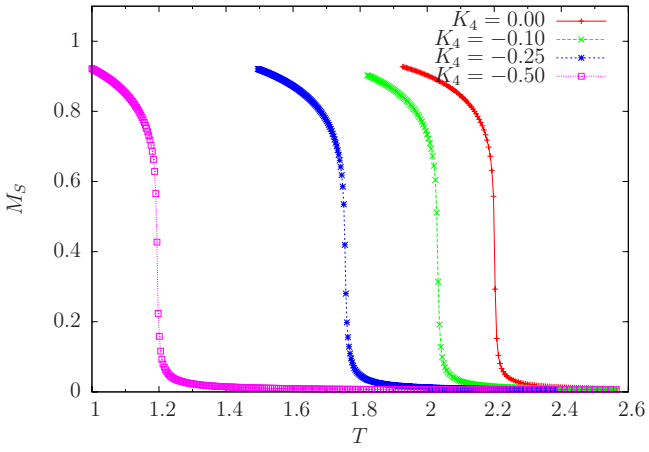

FIG. 14. (Color online) The staggered order parameter, Eq. (3), as a function of temperature T for the classical part of the generalized AT model Eq. (1), with $A=1.0$ and $K^{xy}=0.3$, for various values of $K_4=0.0,-0.1,-0.25,-0.5$, and system size $L=512$.

continuous rotor model with a symmetry-breaking term, provided the symmetry-breaking term is large.

B. M_s, χ_s, and the critical exponents ν and β

Let us now study the order parameter and susceptibility of the order parameter, M_s and χ_s, Eqs. (3) and (4). We have first chosen parameters $A=1.0$, $K^{xy}=0$, and varied K_4, for which the evolution of the specific-heat anomaly is shown in Fig. 5. The results for M_s and χ_s are shown in Figs. 12 and 13, respectively.

We see that the staggered magnetization retains a nonanalytic behavior as in the pure Ising case even for $K_4=-0.5$. This contrasts sharply with the lack of any traces of singular behavior in the specific heat (cf. Fig. 5). From Fig. 13 we see the same trend, namely, that the susceptibility retains a nonanalytic feature even for the largest K_4 values we have considered, and which suffice to completely suppress the singularity in the specific heat.

We have repeated these calculations with $K^{xy}=0.3$. The results are shown in Figs. 14 and 15, with essentially the same results as in Figs. 12 and 13.

We next attempt to estimate the critical exponents ν and β for the model Eq. (1), for the set of parameters $A=1.0$, $K^{xy}=0.1$, and $K_4=-0.25$. (For the same set of parameters but $K^{xy}=0$ and $K_4=0$, see comments below). We base our calculations of these critical exponents on using Binder cumulant Eq. (5) and the scaled staggered magnetization $L^{\beta/\nu}M_s$ [cf. Eq. (3)]. For these computations, we have used up to 3×10^6 sweeps over the lattice for each temperature. In addition, we have used Ferrenberg-Swendsen (FS) multihisto-

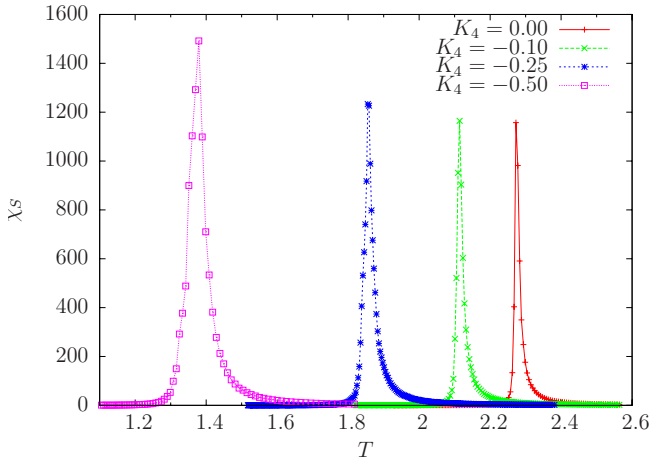

FIG. 13. (Color online) The susceptibility of the staggered magnetization within each unit cell, Eq. (4), as a function of temperature T for the classical part of generalized AT model Eq. (1), with $A=1.0$ and $K^{xy}=0.0$, for various values of $K_4=0.0,-0.1,-0.25,-0.5$, and system size $L=512$. Note that the susceptibility retains the nonanalytical features of the Ising case even for parameters where the specific-heat anomaly is completely suppressed.

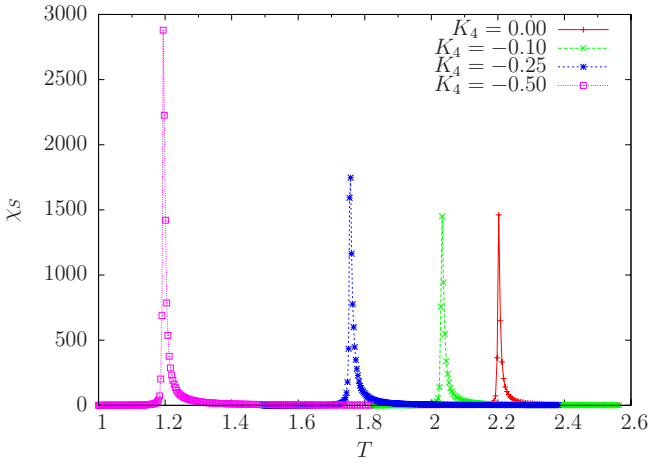

FIG. 15. (Color online) The susceptibility of the staggered magnetization within each unit cell, Eq. (4), as a function of temperature T for the classical part of the generalized AT model Eq. (1), with $A=1.0$ and $K^{xy}=0.3$, for various values of $K_4=0.0,-0.1,-0.25,-0.5$, and system size $L=512$. Note the marked increase in the susceptibility as $-K_4$ is increased, in contrast to the suppression of the anomaly in the specific heat.

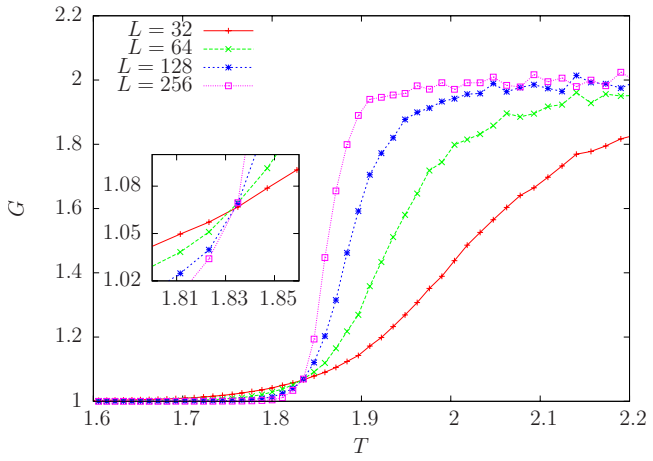

FIG. 16. (Color online) The Binder cumulant G, Eq. (5), as a function of T for model Eq. (1), for $A=1.0$, $K^{xy}=0.1$, and $K_4=-0.25$ for various system sizes, in the absence of Ferrenberg-Swendsen reweighing. The inset shows a blowup of the temperature region where the lines for various system sizes cross, providing an estimate for T_c.

gram reweighting[28] of the raw data for the Binder cumulant in order to improve on the accuracy. The method of computation is described in Sec. II C. In Fig. 16, we show the Binder cumulant for various system sizes as a function of the temperature T without reweighing. The crossing points provide an estimate for T_c. Even in the absence of FS reweighing, there is very little scatter in these crossing points, and T_c is determined with an uncertainty of much less than 1%. With Ferrenberg-Swendsen reweighing, this picture remains, as is seen from Fig. 17 where reweighing is used. An accurate estimate for T_c will turn out to be crucial in the following. Note also that the estimates we get for T_c from the crossing of lines in the Binder cumulant are well in agreement from the somewhat cruder estimates we would obtain

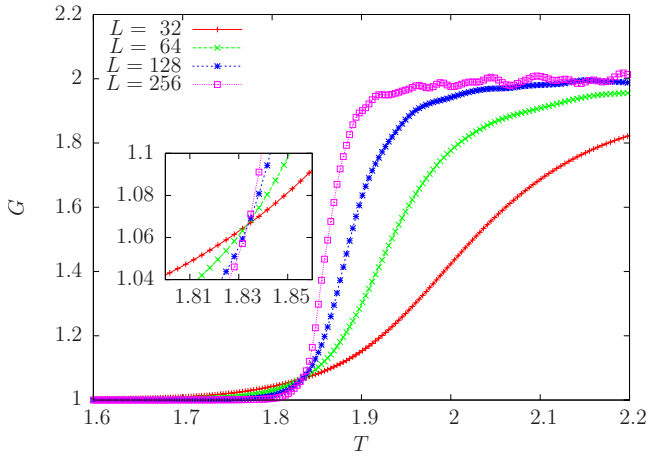

FIG. 17. (Color online) The Binder cumulant G, Eq. (5), as a function of T for model Eq. (1), for $A=1.0$, $K^{xy}=0.1$, and $K_4=-0.25$ for various system sizes, using Ferrenberg-Swendsen reweighing. The inset shows a blowup of the temperature region where the lines for various system sizes cross, providing an estimate for T_c. Note the consistency of the estimate for T_c compared to Fig. 16.

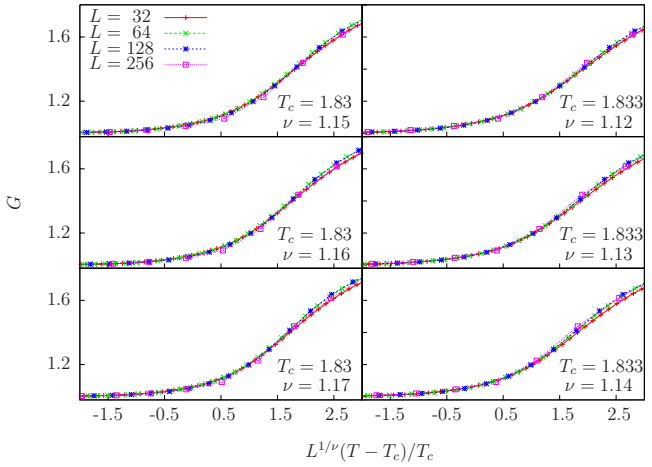

FIG. 18. (Color online) The Binder cumulant G, Eq. (5) as a function of the quantity $L^{1/\nu}(T-T_c)/T_c$, for model Eq. (1), for $A=1.0$, $K^{xy}=0.1$, and $K_4=-0.25$ for various system sizes. Ferrenberg-Swendsen reweighing of the data is used. We have taken estimates for T_c from Fig. 17 and adjusted the correlation length critical exponent ν to achieve the best data collapse. As is seen, the optimal ν is extremely sensitive to the chosen value of T_c.

from determining the temperatures at which the peaks of the staggered susceptibilities occur.

In Fig. 18, we replot the same Binder cumulant, now as a function of the quantity $L^{1/\nu}(T-T_c)/T_c$, using estimates for T_c from Fig. 17 and adjusting ν to get data collapse. While we see that the above computations do not allow us to extract extremely precise values of ν, it does allow us to conclude that the exponent ν is consistent with the values obtained from the Ashkin-Teller model, and that ν appears to be enhanced compared to the 2D Ising value $\nu=1$.

We next compute the quantity $L^{\beta/\nu}M_s$ as a function of the quantity $L^{1/\nu}(T-T_c)/T_c$ to obtain the order-parameter exponent β by using the values of T_c and ν obtained from the scaled Binder cumulant in Fig. 18, and then adjusting β to get data collapse of all magnetization curves for various values of L. The result of this procedure is shown in Fig. 19. Again, from the above we cannot conclude anything with great precision about the exponent β other than saying that it is consistent with the exact values that are known for the Ashkin-Teller model, i.e., Eq. (1) with $K^{xy}=0$.

We have also checked the exponents for the same set of parameters as above except that $K^{xy}=0$. We draw the conclusion that, to the level of precision of the above computations, the exponents are not altered from the Ashkin-Teller case. However, when we repeat the procedure for the same set of parameters as above except that $K^{xy}=0.3$, we find that there is a clear deviation, and that the exponents ν and β definitely do not take Ashkin-Teller values. In particular, we get optimum data collapse for β clearly less than 1/8. From this, we infer that, while the parameter K^{xy} may be perturbatively irrelevant, it may alter the universality class of the phase transition of the model if it is large enough. We also note that the reason that K^{xy} appears to have much less of an effect on the transition when $K_4=0$ compared to when $K_4=-0.25$ is that the latter case represents a frustration of the ferromagnetic Ising ordering that lowers the critical temperature of the

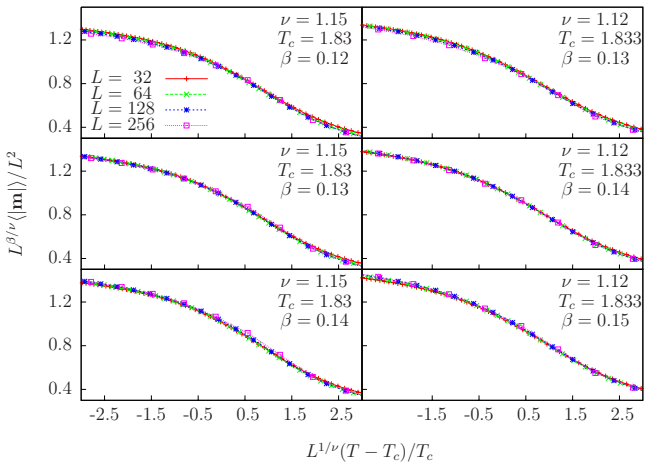

FIG. 19. (Color online) The scaled staggered order parameter $L^{\beta/\nu}M_s$ [cf. Eq. (3)] as a function of the quantity $L^{1/\nu}(T-T_c)/T_c$, for the model Eq. (1), for $A=1.0$, $K^{xy}=0.1$, and $K_4=-0.25$ for various system sizes. Ferrenberg-Swendsen reweighing of the data is used. We have taken estimates for T_c from Fig. 17 and estimates for ν from Fig. 18, and adjusted the order-parameter exponent β to achieve the best data collapse.

system and enhances the effect of introducing K^{xy}, which also frustrates the ferromagnetic Ising ordering, and promotes striped ordering.

Nonuniversality in β due to the presence of the parameter K_4 in the problem means that β in principle should vary slightly as we cross the pseudogap line vertically in the (x,T)-phase diagram of high-T_c cuprates as the doping is varied, if we assume that the parameters of the effective model Eq. (1) varies as we move along the pseudogap line. In particular, a variation in β with K_4 is clearly seen from Fig. 12 although we have not performed a detailed finite-size scaling analysis to determine β as a function of K_4. We also note from Fig. 4 that introduction of K^{xy} does not change the universality class of the transition when $K_4=0$. We may therefore quite reasonably assume that the presence of K^{xy} does not change the Ashkin-Teller universality class of the phase transition when K_4 is present, provided K^{xy} is not too large. We may then deduce that, for negative K_4, we will have $-2<\alpha<0$, $1/8<\beta<1/4$, and $7/4<\gamma<7/2$. A suppression of the specific-heat anomaly as seen for the case $K_4=-0.25$ puts us at $\alpha\approx-0.37$, $\beta\approx0.15$, and $\gamma\approx2.07$. The weak variation in the exponent β from the Ising value 1/8 is due to the near cancellation of the rather large, but opposite, variations in the specific-heat exponent α and the susceptibility exponent γ, consistent with the scaling law $\alpha+2\beta+\gamma=2$. It is precisely the large variation in α that wipes out the specific-heat anomaly that also produces a large enhancement of the susceptibility of the staggered orbital magnetization, see Fig. 3.

C. Comparison of calculated specific heat with experiments

We use the results in Figs. 4–11 to estimate the peak value of the specific-heat bump expected due to the transition to see why it may be unobservable in experiments performed so far. In comparing with experiments, the following should be borne in mind. The ordering below the transition temperature is three dimensional (3D). Hence, the observed specific heat will be that of the form calculated above as temperature is decreased toward T^*, followed by a singularity characteristic of the 3D Ising model near T^* and below it. However, the integrated value of specific heat divided by T under the singularity is only a fraction of the total entropy due to the loop order degrees of freedom. As we discuss below, the latter itself is more than an order of magnitude smaller than the entropy due to fermionic excitations in the same temperature range.

The area $\int[C_v(T)/T]dT$ over all temperatures in each of the curves in Figs. 4–11 is $2\ln(2)k_B$/unit cell, reflecting that the calculations are performed for 2 Ising degrees per unit cell. Given that the ordered moment due to orbital currents is estimated in neutron-scattering experiments to be $10^{-1}\mu_B$/unit cell, the integrated value is expected to be $2\ln(2)k_B$/unit cell multiplied by $O(10^{-2})$. To compare with experiments, we may consider calculations for the case $K^{xy}=0$ and $|K_4/K_l|$ between, say 0.25 and 0.5. The peak value of the specific heat from Figs. 4–11 is then expected to be less than $0.5\times10^{-2}k_B$ per unit cell or less than about 0.05 J/mol/deg. This should be compared with the measured specific heat,[29] which at about 200 K is about 200 J/mol/deg. In Ref. 29, the electronic specific heat is estimated by subtracting the specific heat for a similar nonmetallic compound to be about 2 J/mol/deg. Therefore, the bump has a peak which is 3–4 orders of magnitude smaller than the total specific heat, and 1–2 orders of magnitude smaller than even the deduced electronic specific heat. Given that the specific-heat bump is spread out over temperatures of $\mathcal{O}(2T^*)$, it is not surprising that with pseudogap temperatures of $\mathcal{O}(200)$ K or higher, it has gone undetected. There are underdoped cuprates with lower T^*, in which a bump in the specific heat with magnitude of order that suggested here is claimed[30] to be observed.

IV. UNIFORM SUSCEPTIBILITY

Just as the onset of antiferromagnetic spin order has a weak parasitic nonanalytic effect on the uniform magnetic susceptibility, the onset of loop-current orbital magnetic order may be expected to have a similar effect on the uniform magnetic susceptibility. Such an effect has indeed been measured recently in careful studies across $T^*(x)$.[9]

Since the uniform magnetization is a parasitic effect on the staggered magnetization, we can calculate its temperature dependence by a Landau theory in which we consider the free energy for the staggered magnetization but consider the minimal coupling of the uniform magnetization to the staggered magnetization. Let M_s be the staggered magnetization and $\langle M\rangle$ be the thermal average of the uniform magnetization in the presence of an external field H. Let $F_0(M_{s0})$ be the free energy for the M_s in the absence of an external magnetic field H. Quite generally, the leading terms in the free energy are given by

$$F = F_0(M_s) + \frac{M^2}{2\chi_0} - MH + \frac{C}{2}M_s^2M^2 + \ldots . \tag{7}$$

Here, C is a coefficient which gives the competition between the staggered and uniform magnetizations. The sign of C is

positive if, as is reasonable, the staggered magnetization decreases when the uniform magnetization increases, and vice versa.

This form of the free energy gives correct answers only in the regime in which the staggered susceptibility is small and therefore is not valid very close to the transition. Also, the susceptibility calculated is for magnetic field parallel to the direction of sublattice magnetization. In the simplest theory, this direction is perpendicular to the Cu-O planes. In the experiments,[5] an angle closer to $\pi/4$ has been deduced for which some theoretical justifications are provided.[16,31] Since the experiments are done in powder samples, we will ignore this issue for the present.

Let $\chi_{s0} \equiv (\partial^2 F_0/\partial M_{s0}^2)^{-1}$ be the order-parameter susceptibility, which is calculated above. The subscript 0 in χ_{s0} indicates the quantity in the absence of $\langle M \rangle$. χ_0 is the uniform susceptibility in the absence of M_s. Then in the presence of $\langle M \rangle$, induced by the external field H, the condition

$$\frac{\partial F}{\partial M} = 0, \tag{8}$$

gives

$$\frac{\langle M \rangle}{\chi_0} - H + C\langle M \rangle \langle M_s^2 \rangle = 0. \tag{9}$$

This gives $\langle M \rangle \equiv \chi H$ in linear response (i.e., low H), with

$$\chi = \frac{\chi_0}{1 + C\chi_0 \langle M_s^2 \rangle}. \tag{10}$$

Here, $\langle M_s^2 \rangle$ is the thermodynamic squared magnetization in the presence of $\langle M \rangle$, and χ is the uniform susceptibility. We may write Eq. (10) as

$$\chi = \frac{\chi_0}{1 + C\chi_0(\langle M_s \rangle^2 + T\chi_s)}. \tag{11}$$

Also, quite generally, the order-parameter susceptibility is

$$\chi_s^{-1} = \frac{\partial^2 F}{\partial M_s^2} = \chi_{s0}^{-1} + C\langle M^2 \rangle = \chi_{s0}^{-1} + CT\chi. \tag{12}$$

This gives

$$\chi_s = \frac{\chi_{s0}}{1 + CT\chi\chi_{s0}}. \tag{13}$$

Thus, using Eqs. (12) and (13), we may write χ in terms of known quantities χ_0 and χ_{0s} to obtain

$$CT\chi_{s0}\chi^2 + \chi - \chi_0 = 0. \tag{14}$$

For $T \gg T_c$, where the above treatment is valid, we have $4CT\chi_{s0}\chi_0 \ll 1$ so that

$$\chi \approx \chi_0 - CT\chi_{s0}\chi_0^2, \quad (T - T_c)/T_c \gg 1. \tag{15}$$

The uniform susceptibility is therefore predicted to decline from its constant Pauli value at far above T_c in the same range that χ_{s0} shows a rise. We suggest that the observed slow decrease in $\chi(T)$ for temperatures well above T^* be fitted to such a form.

Well below T_c, the model behaves as an Ising model. Therefore, the contribution of the ordered moments to the uniform susceptibility approaches zero exponentially as $T \to 0$.

A. Mean-field jump in $d\chi/dT$ at T_c

In a mean-field calculation χ_{s0} does not change above T_c. There is, however, a jump in $d\chi/dT$ expected at T_c. The experimental results have been quantified by such a jump.[9] To compare with available experimental results, we approximate Eq. (12) as

$$\chi \approx \chi_0 - C\chi_0^2 \langle M_s \rangle^2, \tag{16}$$

so that

$$\frac{d\chi}{dT} = -C\chi_0^2 \frac{d\langle M_s \rangle^2}{dT}. \tag{17}$$

Here, a temperature independent χ_0 is assumed. We now need to know the right side of Eq. (17). This may be estimated as follows. Returning to Eq. (7), we may write $F_0(M_s)$ as

$$F_0(M_s) = \tilde{\alpha}/2 \frac{(T - T_0^*)}{T_0^*} M_s^2 + \frac{\beta}{4} M_s^4 + \ldots. \tag{18}$$

This defines the transition temperature T_0^* in the absence of an external magnetic field H, i.e., for $M = 0$. It also defines an inverse susceptibility α for M_s, which we expect to be of the same order as to the inverse of the density of states at the Fermi surface, or equivalently of order χ_0^{-1}. Combining Eq. (18) with the third term in Eq. (7), we see that a finite M leads to a decrease in the transition temperature δT^*, with

$$\frac{\delta T^*}{T^*} \approx CM^2/\tilde{\alpha}. \tag{19}$$

Note also that

$$M_s^2 \approx M_s(0)^2 \frac{(T_0^* - T)}{T_0^*}, \tag{20}$$

where $M_s(0)^2$ is the zero-temperature value of M_s^2. Using this in Eq. (17), the jump in the derivative of the susceptibility at T^* is given by

$$\frac{T_0^*}{\chi_0} \frac{d\chi}{dT} = CM_s(0)^2 \chi_0. \tag{21}$$

Now we need an estimate of $CM_s(0)^2$. This can be obtained from Eq. (19) if we note that the transition temperature will be reduced to zero, i.e., $\frac{\delta T^*}{T^*} = 1$, for some magnetization $M*$. The magnitude of $M*$ has to be the same order as $M_s(0)$ at zero field. Therefore

$$CM_s(0)^2/\tilde{\alpha} \approx 1. \tag{22}$$

Using this above, the jump in $d\chi/dT$ at T^* is given by

$$\frac{T_0^*}{\chi_0} \frac{d\chi}{dT} \approx \tilde{\alpha}\chi_0 \approx 1, \tag{23}$$

where we have used the estimate for $\tilde{\alpha}$ estimated earlier.

In the experiments reported in Ref. 9, a value of $\frac{T_0^*}{\chi_0}\frac{d\chi}{dT}$ between 0.2 and 0.3 has been deduced. This should be considered in good agreement with the estimate of O(1). The weak assumptions in the analysis above are the lack of knowledge of the numerical constant between $\tilde{\alpha}$ and χ_0^{-1}, and the unknown numerical constant on the right-hand side of Eq. (22), instead of one. However, they cannot be off by more than an order of magnitude from those assumed. In a mean-field calculation χ_{s0} does not change above T_c. There is, however, a jump predicted in $d\chi/dT$ expected at T_c.

V. SUMMARY

We have studied the evolution of the specific heat and other thermodynamic properties in an effective theory of fluctuating orbital currents in high-T_c cuprates. The motivation for the work has been to see if the finite-temperature breakup of a proposed ordering associated with a loop-current pattern is consistent with both the existence of an order parameter in the pseudogap phase below a temperature $T^*(x)$, and with an *absence* of an observed singularity in the specific heat and a weak singular feature in the uniform magnetization at $T^*(x)$. This is a first step toward investigating, through quantum Monte Carlo simulations, whether the quantum breakup of such order gives rise to quantum critical fluctuations that could possibly explain the anomalous transport properties in the normal state of these compounds, as has been proposed in analytic calculations.[3] In this paper, we have shown that the effective-field theory of the particular proposed order of orbital currents within a CuO_2 plane passes this test by destroying the order while exhibiting no divergence in the specific heat. Instead, we have found bumps which we have estimated to be of a magnitude that are unobservable in experiments done so far. Moreover, we find a uniform magnetic susceptibility with a nonanalytic behavior as a function of temperature as the phase transition is crossed. From a technical point of view, a principal result of our calculations is that the anisotropy considered in the Ashkin-Teller model as well as the next-nearest-neighbor interactions, in the range of parameters considered, are irrelevant perturbations.

ACKNOWLEDGMENTS

This work was supported by the Norwegian Research Council Grants No. 158518/431 and No. 158547/431 (NANOMAT), and Grant No. 167498/V30 (STORFORSK). The authors acknowledge communications and discussions with V. Aji, K. Børkje, E. H. Hauge, B. Leridon, J. Linder, A. Shekhter, Z. Tesanovic, and M. Wallin.

[1] C. M. Varma, Phys. Rev. B **55**, 14554 (1997); Phys. Rev. Lett. **83**, 3538 (1999).
[2] M. E. Simon and C. M. Varma, Phys. Rev. Lett. **89**, 247003 (2002); C. M. Varma, Phys. Rev. B **73**, 155113 (2006).
[3] V. Aji and C. M. Varma, Phys. Rev. Lett. **99**, 067003 (2007).
[4] C. M. Varma, P. B. Littlewood, S. Schmitt-Rink, E. Abrahams, and A. E. Ruckenstein, Phys. Rev. Lett. **63**, 1996 (1989).
[5] B. Fauqué, Y. Sidis, V. Hinkov, S. Pailhes, C. T. Lin, X. Chaud, and P. Bourges, Phys. Rev. Lett. **96**, 197001 (2006).
[6] H. A. Mook, Y. Sidis, B. Fauqué, V. Balédent, and P. Bourges, Phys. Rev. B **78**, 020506 (2008).
[7] Y. Li, V. Balédent, N. Bari, Y. Cho, B. Fauqué, Y. Sidis, G. Yu, X. Zhao, P. Bourges, and M. Greven, Nature (London) **455**, 372 (2008). These authors find, through polarized neutron scattering, the same magnetic order setting at $T^*(x)$ in Hg cuprates as found in Refs. 5 and 6 in $YBa_2Cu_3O_{6+\delta}$.
[8] A. Kaminski, S. Rosenkranz, H. M. Fretwell, J. C. Campuano, Z. Li, H. Raffy, W. G. Cullen, H. You, C. G. Olson, C. M. Varma, H. Hochst, Nature (London) **416**, 610 (2002). These authors discovered a symmetry breaking in circularly polarized angle-resolved photoemission experiments measurements in underdoped the high-temperature superconductor BISCCO compounds at $T^*(x)$, which was analyzed in Ref. 2 to be consistent with loop-current order of the form shown in Fig. 1.
[9] B. Leridon, P. Monod, and D. Colson, arXiv:0806.2128 (unpublished).
[10] K. Børkje and A. Sudbø, Phys. Rev. B **77**, 092404 (2008).
[11] A. Sudbø, S. Schmitt-Rink, and C. M. Varma, Phys. Rev. B **46**, 5548 (1992).
[12] A. Sudbø, C. M. Varma, T. Giamarchi, E. B. Stechel, and R. T. Scalettar, Phys. Rev. Lett. **72**, 3292 (1994).
[13] A. W. Sandvik and A. Sudbø, Phys. Rev. B **54**, R3746 (1996).
[14] M. Greiter and R. Thomale, Phys. Rev. Lett. **99**, 027005 (2007); R. Thomale and M. Greiter, Phys. Rev. B **77**, 094511 (2008).
[15] M. S. Hybertsen, E. B. Stechel, M. Schluter, and D. R. Jennison, Phys. Rev. B **41**, 11068 (1990).
[16] C. Weber, F. Mila, and T. Giamarchi, Phys. Rev. Lett. **102**, 017005 (2009).
[17] H. C. Lee and H.-Y. Choi, Phys. Rev. B **64**, 094508 (2001).
[18] S. Chakravarty, R. B. Laughlin, D. K. Morr, and C. Nayak, Phys. Rev. B **63**, 094503 (2001).
[19] K. Børkje, Ph.D. thesis, Norwegian University of Science and Technology, 2008.
[20] J. Ashkin and E. Teller, Phys. Rev. **64**, 178 (1943).
[21] R. J. Baxter, *Exactly Solved Models in Statistical Mechanics* (Academic, London, 1982).
[22] Anisotropy is generic to bond variables, which, unlike site variables, have *directionality*. In the present paper, we treat a problem in the particle-hole channel. See however also A. Melikyan and Z. Tesanovic, Phys. Rev. B **71**, 214511 (2005), and Z. Tesanovic, Nat. Phys. **4**, 408 (2008). These authors treat a problem in the particle-particle channel, namely, the case of a phase-fluctuating lattice *d*-wave superconductor where the phase of the *d*-wave superconducting order parameter is a bond variable.
[23] N. Metropolis, A. W. Rosenbluth, M. N. Rosenbluth, A. H. Teller, and E. Teller, J. Chem. Phys. **21**, 1087 (1953).
[24] W. K. Hastings, Biometrika **57**, 97 (1970).
[25] J. V. José, L. P. Kadanoff, S. Kirkpatrick, and D. R. Nelson, Phys. Rev. B **16**, 1217 (1977).
[26] L. P. Kadanoff and A. C. Brown, Ann. Phys. **121**, 318 (1979).

[27] J. Smiseth, E. Smørgrav, F. S. Nogueira, J. Hove, and A. Sudbø, Phys. Rev. B **67**, 205104 (2003). We have in fact attempted to use the scaling analysis of the above paper to model Eq. (1). However, the double bump in the specific heat for larger $|K_4|$ and system sizes in the range $L \leq 128$ means that, in order to use the method of the above reference, impractically large system sizes $L > 256$ are required for the finite-size scaling analysis. Since a precise numerical determination of α is not the main goal of this paper, we have not attempted this.

[28] A. M. Ferrenberg and R. H. Swendsen, Phys. Rev. Lett. **63**, 1195 (1989).

[29] J. W. Loram, K. A. Mirza, J. R. Cooper, and W. Y. Liang, Phys. Rev. Lett. **71**, 1740 (1993).

[30] T. Matsuzaki, N. Momono, M. Oda, and M. Ido, J. Phys. Soc. Jpn. **73**, 2232 (2004).

[31] V. Aji and C. M. Varma, Phys. Rev. B **75**, 224511 (2007).